Second harmonic generation in one-dimensional photonic crystals: optimization procedure

Centini, Marco, D'Aguanno, Giuseppe, Sciscione, Letizia, Sibilia, Concita, Bertolotti, Mario, et al.

Marco Centini, Giuseppe D'Aguanno, Letizia Sciscione, Concita Sibilia, Mario Bertolotti, Michael Scalora, Mark J. Bloemer, "Second harmonic generation in one-dimensional photonic crystals: optimization procedure," Proc. SPIE 5450, Photonic Crystal Materials and Nanostructures, (15 September 2004); doi: 10.1117/12.545651

Event: Photonics Europe, 2004, Strasbourg, France

Second Harmonic Generation in one dimensional Photonic Crystals: Optimization Procedure.

Marco Centini[*a,b], Giuseppe D'Aguanno[a,b], Letizia Sciscione[a], Concita Sibilia[a], Mario Bertolotti[a], Michael Scalora[b], and Mark J. Bloemer[b]
[a]INFM at Dipartimento di Energetica, Università di Roma "La Sapienza", Via Scarpa 16, 00161 Roma, Italy;
[b]U.S. Army Aviation and Missile Command, Weapon Sciences Directorate, AMSMI-RD-WS-ST Redstone Arsenal, Huntsville, Alabama 35898-5000

ABSTRACT

We present a new concept for efficient second harmonic generation that is based upon the interference of counter-propagating waves in multilayer structures. We show that phase matching and quasi phase matching are not always necessary conditions to provide optimized nonlinear frequency conversion efficiency

Keywords: Non-Linear frequency conversion, multilayer stacks.

1. INTRODUCTION

Phase-Matching (PM) or quasi phase-matching condition are usually required as specific starting point in any method for generating an efficient second harmonic (SH) [1]. Further studies showed that it is possible to achieve PM in infinite [2] and finite [3] multilayer stacks called One Dimensional Photonic Crystals (1D-PC). Recent experiments on these structures (i.e. PM AlGaAs/AlO_x multilayers) confirmed that the conversion efficiency scales as L^6 where L is the length of the 1D-PC [4]. Dumeige et al. predict that a 55 period, L=15μm, AlGaAs/AlO_x structure will have a 10% conversion efficiency for a fundamental peak power of 1KW. The spectral bandwidth of the enhancement is 0.25 nm and comparable with pulse durations of 15 ps or longer. Cascading several 1D-PC in series can be used to expand bandwidths [5].

As shown in our earlier publication [3], PM conditions can be fulfilled in 1D-PC whose alternating layers are of optical thickness $\lambda/2$ and $\lambda/4$ with the nonlinearity in the high refractive index, half-wave layers. Optimum PM can be achieved both with a proper choice of the layer thickness and well juxtaposing the fundamental (FF) and second harmonic (SH) frequency in the linear spectrum. FF is tuned to the first transmission resonance near the lowest energy stop band and the SH field at the second transmission resonance next to the second order stop band (see Fig. 1 solid line arrows). The PM conditions for a 1D-PC force the SH to be at the 2nd transmission resonance where the mode density is not at its highest value in fact photon density of modes and the field enhancements are largest near the stop bands. Detuning from the PM condition degrades the conversion efficiency as predicted in reference [3]. Nevertheless, the aim of this work is to show that, under appropriate conditions, nonphase-matched 1D-PC designs can yield a further order of magnitude improvement in the conversion efficiency with respect to PM state of art designs. The enhancement in nonphase-matched SH generation is due to a combination of high photon mode density and a contribution to fast varying interference terms which average to near zero if the thickness of the nonlinear layer is half-wave or greater. This is unique to a finite size 1D-PC since neither bulk material nor the smallest cavity, ie. $\lambda/2$, will display this type of contribution to nonlinear dynamics from the interference of counter-propagating waves.

Photonic Crystal Materials and Nanostructures, edited by Richard M. De La Rue, Pierre Viktorovitch, Clivia M. Sotomayor Torres, Michele Midrio, Proceedings of SPIE Vol. 5450 (SPIE, Bellingham, WA, 2004) · 0277-786X/04/$15 · doi: 10.1117/12.545651

2. EFFECTIVE NONLINEAR COEFFICIENT

An analytic expression for the conversion efficiency for a generic layered structure of finite length composed of non-absorbing media was derived by using a multiple scale approach [6]. Considering undepleted pump approximation the conversion efficiency in a finite structure of length L is proportional to the square modulus of an effective coupling coefficient, defined as:

$$\tilde{d}_{eff} = \frac{1}{L}\int_0^L \chi^{(2)}(z)\Phi_{\omega}^2(z)\Phi_{2\omega}^*(z)dz \,. \qquad (1)$$

Where $\Phi_\omega(z)$ and $\Phi_{2\omega}(z)$ are the complex, linear field profiles normalized with respect to a unitary input field and the electric field inside the structure can be written as: $E_{i\omega}(z) = E_{i\omega}^0\left(\Phi_{i\omega}(z) + c.c.\right)$, where (i=1,2), and $E_{i\omega}^0$ is the amplitude of input field. Unlike the d_{eff} defined for studying nonlinear propagation in waveguides [7-8], the $\tilde{d}_{eff}$ in Eq.(1) is a complex quantity and it contains information regarding field distribution and localization, as well as contributions to the conversion efficiency coming from the PM conditions.

In the specific case of an SH generation in a *infinite* periodic structure the expression of the coupling coefficient can be calculated using the Bloch theory, so that the complex, linear field profiles can be written:

$$\Phi_{j\omega}(z) = f_{j\omega}(z)e^{ik_\beta(j\omega)z} \text{ where j=1,2,} \qquad (2)$$

here $f_{j\omega}(z)$ is a periodic function whose period is the thickness of the unit cell Λ, i.e.:

$$f_{j\omega}(z+\Lambda) = f_{j\omega}(z) \qquad (3)$$

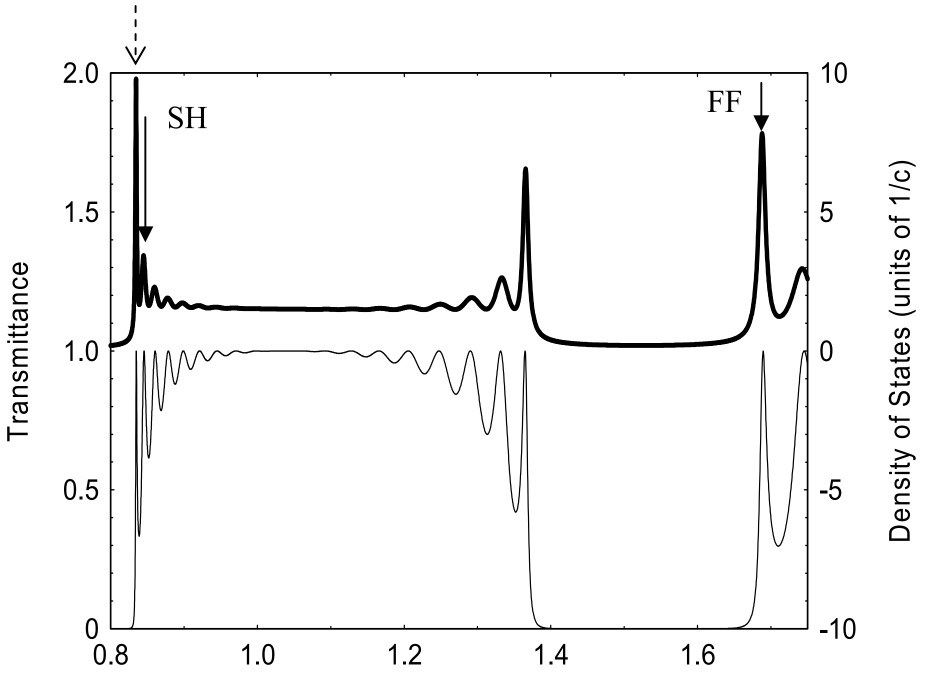

Figure 1: Transmission spectrum and density of states (thick line) vs wavelength at normal incidence for a 20 period mixed half-wave/quarter-wave stack. FF and SH tuning are indicated by the arrows.

and $\Delta k_\beta = k_\beta(2\omega) - 2k_\beta(\omega)$ is the Bloch wave-vector mismatch. The expression of the coupling coefficient becomes:

$$\tilde{d}_{\text{eff}} = I_{u.c.} \sum_m \delta(\Delta k_\beta - \frac{2\pi}{\Lambda} m); \quad \text{(m=0,1,2,...)}, \tag{4}$$

$I_{u.c.}$ is the overlap integral calculated over the unit cell containing all the information about the geometry (layer thickness, refractive index contrast), amount and position of the nonlinear material inside the unit cell and fields' overlap. We can think of $I_{u.c}$ as a form factor and it can be described by the formula:

$$I_{u.c.} = \frac{1}{\Lambda} \int_0^\Lambda \chi^{(2)}(z) f_\omega^2(z) f_{2\omega}^*(z) e^{i\Delta k_\beta z} dz \tag{5}$$

For a finite structures, $f_{j\omega}(z)$ are no longer periodic over the unit cell because of the break of the transnational symmetry. Indeed, the truncation of the periodicity is responsible of the appearance of sharp resonant peaks in the transmission band as well as field localization effects. In this case the expression of the $\tilde{d}_{eff}$ reads:

$$\tilde{d}_{eff} = \frac{1}{N} \sum_{j=0}^{N-1} \left[\frac{1}{\Lambda} \int_0^\Lambda \chi^{(2)}(z) f_\omega^2(j\Lambda + z) f_{2\omega}^*(j\Lambda + z) e^{i\Delta k_\beta z} dz \right] e^{i(\Delta k_\beta \Lambda) j} = \frac{1}{\mathrm{N}} \sum_{\mathrm{j}=0}^{\mathrm{N-1}} \mathrm{I}_{\mathrm{j}}^{\mathrm{u.c.}} e^{i(\Delta k_\beta \Lambda) j}; \tag{6}$$

Thus, we can deduce that every unit cell gives a different contribution to the overlap integral. The value of the overall sum remains inscrutable and it can be read as the superposition of N sources having different amplitudes and phases. Nevertheless, Eq.(6) suggests that standard theories of quasi-phase matching based on Bloch's quasi-momentum conservation may fail in a wide range of cases. In fact, conversion efficiency can be further enhanced by at least one order of magnitude compared to a phase matched case.

3. NUMERICAL RESULTS

We choose a structure with mixed quarter-wave/half-wave geometry and 20 periods. The nonlinear material ($\lambda/4$ optical thickness) has a refractive index $n_2(\omega_{FF}) = 1.428$ at the FF frequency. For simplicity, the linear material ($\lambda/2$ optical thickness) is assumed to be air, with $n_1=1$, with a reference wavelength used to calculate the optical paths of the layers is 1 μm, corresponding to an angular frequency $\omega_0 = 1.88 \cdot 10^{15}$ s^{-1}. This simple geometrical arrangement allows us to rather easily tune the FF and SH fields to the two resonance peaks each located near two consecutives band gaps of the transmission spectrum (assuming normal incidence), where field localization effects are maximized. The linear spectrum at normal incidence is shown in Fig.(1) and the FF is tuned at the first order band edge resonance ($\lambda_{FF}=1.69$ μm which corresponds to $\omega_{FF}=0.592\omega_o$, as labeled by the arrow). After fixing the layer thickness, dispersion by varying the index of refraction at the SH frequency ($\omega_{SH} = 1.184\omega_o$) may be added to tune the field to any desired frequency near the band edge (an increase of the value of $n_2(\omega_{SH})$ redshifts the band structure). Varying the refractive index in this fashion can be thought as an artifice but it allows us to find the optimized parameters as a function of one degree of freedom and to distinguish the competing roles played by phase matching and by local field enhancement during the conversion process.

In Fig.(2) we depict the polar plot containing modulus and angular phase of the N addends of Eq. (6) when the high index material is given suitable dispersion in two different situations. For the first one $n_2(\omega_{SH})=1.676$ and so the SH is tuned to the first band edge resonance (see Fig (1) dashed arrow). The corresponding curve is in Fig. (2a) labeled by asterisks. In the same figure we compare these results to the ones (circles) obtained when effective phase matching conditions are achieved by choosing $n_2(\omega_{SH})=1.616$ (SH is tuned at the second resonance peak as explained in Ref.[3]). We note that in the latter case (circles) the amplitude of the N addends is smaller because the density of modes for the SH field is smaller, i.e., fields localization is weaker. Moreover, they appear to be more out of phase, and the overall sum is not maximized. In other words, the phases of the addends are spread over a wider angular range. Indeed, the square modulus of the sum is one order of magnitude smaller than the one calculated for the previous case. Therefore, according to our model, the expected conversion efficiency is one order of magnitude lower compared to the non-phase matched case.

For completeness, we consider a structure where phase matching conditions dominate. We, only, invert the geometry taking the nonlinear layer to have optical thickness $\lambda/2$ and the linear layer $\lambda/4$. We performed the same calculation for this structure. In this way, we could compare the behavior of two similar structures made with the same materials and having the same number of periods. The results are shown in fig. (2b). Once again the asterisks represent the case in which the second harmonic field is tuned at the first resonance and the circles represent the phase matched case. As expected for this structure fulfillment of PM conditions leads to optimum conversion efficiency although it is one order of magnitude lower than the one obtained with the previous structure in the non phase matched regime. Thus, by simply changing the filling ratio of the nonlinear layer inside the unit cell we switched from a regime in which PM conditions rule the nonlinear dynamics to a regime where fields'overlap dominate.

In Fig.(3a) we plotted the value of the square modulus of $\tilde{d}_{eff} / \chi^{(2)}$ as a function of the refractive index $n_2(\omega_{SH})$ when the pump field remains tuned at the band edge resonance (thick solid line). As previously outlined in the *effective index theory* (Ref.[3]), maximum conversion efficiency is expected to be achieved when the second harmonic field is tuned at the second resonance and the ratio $\left|\tilde{d}_{eff} / \chi^{(2)}\right|^2$ is described by the function $|\mathrm{sinc}(\Delta k_{eff}L/2)|$^2 [2] (see Fig. (3a) (thin line)).

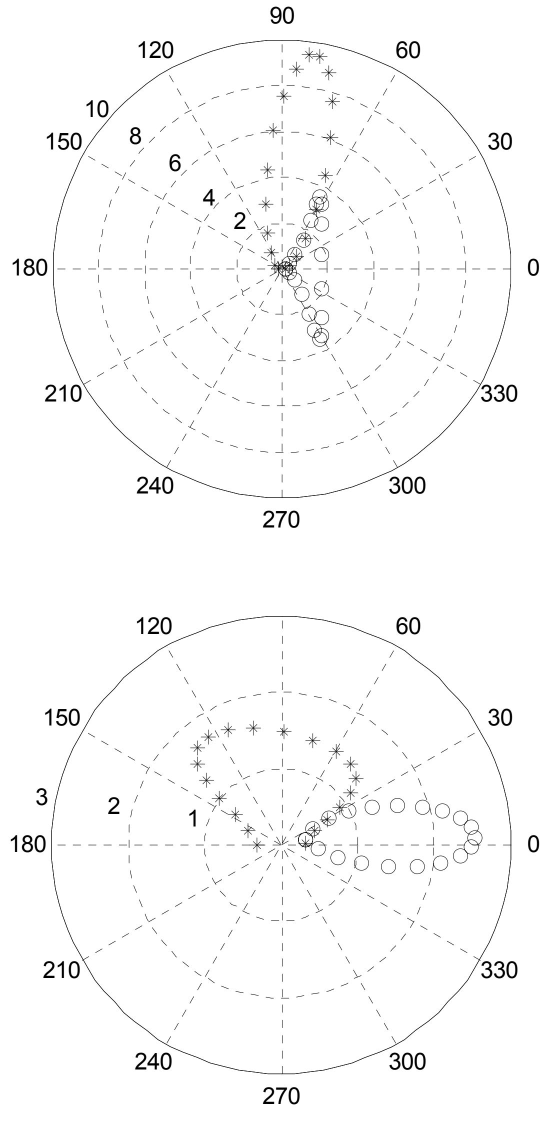

Figure 2: Polar plots of the N addends of Eq(6) when phase matching conditions are achieved (circles) and when both FF and SH fields are tuned at the band edge resonance(asterisks). The non linear material layers optical thickness is: (a) $\lambda_0/4$; (b) $\lambda_0/2$.

By the comparison of the two curves we note that there is only a relative maximum of $\left|\tilde{d}_{eff} / \chi^{(2)}\right|^2$ when effective PM is fulfilled, instead an absolute maximum is achieved when the second harmonic field is tuned to the first band edge resonance (note that the amount of dispersion introduced, i.e., $n_2(\omega_{SH})$- $n_2(\omega_{FF})$ =0.248, is not atypical of common materials). In this case, the effective mismatch is Δn_{eff}=0.06 and the conversion efficiency will be one order of magnitude greater compared to the case of exact, effective PM. Finally we show the tuning curve ($\left|\tilde{d}_{eff} / \chi^{(2)}\right|^2$ vs. FF wavelength) for our optimized structure (Fig 3b). At λ_{FF}=1.69 μm, the enhancement factor is more than 3 orders of magnitude larger compared to the out-of-resonance case, with a usable bandwidth of approximately 4nm.

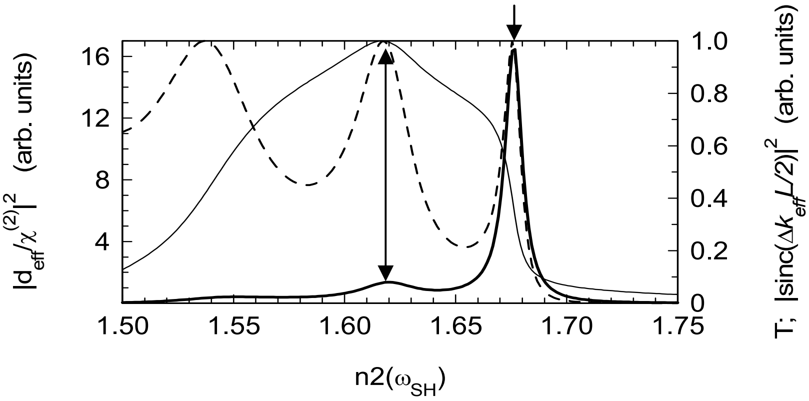

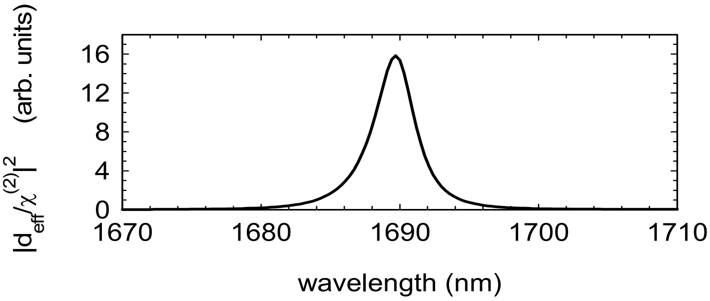

Figure.3: **a)** (thick solid line): Enhancement factor $\left|\tilde{d}_{eff} / \chi^{(2)}\right|^2$ vs. $n_2(\omega_{SH})$; (thin solid line): Phase matching contribution given by the expression: |sinc(Δk_{eff}L/2)|^2 vs. $n_2(\omega_{SH})$. (right y axis); (dashed line): SH transmission as a function of $n_2(\omega_{SH})$. (left y axis). **b)** $\left|\tilde{d}_{eff} / \chi^{(2)}\right|^2$ vs. FF wavelength for the optimized 20 period structure, δh=0.175 μm and δl=0.5 μm. The parameters used are n_l=1, $n_2(\lambda)=1.333 + 0.28/\lambda^2 - 0.025/\lambda^4$ with λ expressed in μm.

4. ANALITICAL INTERPRETATION

To provide a qualitative interpretation of this phenomenon we decompose the complex linear field profiles as a superposition of forward and backward waves in each layer:

$$\Phi_{\omega}^{j,m}(z) = \left[A_{j,m} e^{ik_0 n_m(\omega)(z-z_{j,m})} + B_{j,m} e^{-ik_0 n_m(\omega)(z-z_{j,m})} \right]; \tag{7a}$$

$$\Phi_{2\omega}^{j,m}(z) = \left[C_{j,m} e^{i2k_0 n_m(2\omega)(z-z_{j,m})} + D_{j,m} e^{-i2k_0 n_m(2\omega)(z-z_{j,m})} \right]; \tag{7b}$$

where j=1:N, m=1,2 , *A, B, C,*and *D,* are constants that can be calculated by imposing boundary conditions at every interface.Substituting Eqs.(7) into the expression for the coupling coefficient, taking $\chi^{(2)}(z)=0$ everywhere except within the nonlinear layers, and performing the integral in each layer we obtain:

$$\tilde{d}_{eff}=\frac{\chi^{(2)}dh}{L}\Bigg[sinc\left(k_0\Delta n_2 dh\right)\sum_{j=0}^{N}\left(A_{j,2}^2C_{j,2}^*e^{ik_o\Delta n_2 dh}+B_{j,2}^2D_{j,2}^*e^{-ik_o\Delta n_2 dh}\right)+$$

$$+2sinc\left(k_0 n_2(2\omega)dh\right)\sum_{j=0}^{N}A_{j,2}B_{j,2}\left(C_{j,2}^*e^{ik_o n_2(2\omega)dh}+D_{j,2}^*e^{-ik_o n_2(2\omega)dh}\right)+ \qquad (8)$$

$$+sinc\left(2k_0(n_2(2\omega)-\Delta n_2/2)dh\right)\sum_{j=0}^{N}\left(A_{j,2}^2D_{j,2}^*e^{-i2k_o(n_2(2\omega)-\Delta n_2/2)dh}+B_{j,2}^2C_{j,2}^*e^{i2k_o(n_2(2\omega)-\Delta n_2/2)dh}\right)\Bigg]$$

where $\Delta n_2=n_2(2\omega)-n_2(\omega)$. We note that the relevance of the three terms on right hand side (RHS) of Eq.(8) depends on the nonlinear layer thickness dh because of the *sinc* functions. This is due to the fact that there is no local phase matching due to the natural material dispersion of the high index material. As a result, field overlap cannot be maximized over an arbitrary nonlinear layer of length dh. In particular, the first term is related to the material index mismatch while the second and third terms give an almost zero contributions if the optical thickness of the nonlinear layer is longer than approx λ/2 and λ/4 respectively. Those fast varying terms arise from interference of counter-propagating waves inside the structure generated by multiple reflections at the interfaces, and are generally neglected in bulk or microcavity theories. Nevertheless, in the case we showed, terms in Eq. 8 can not generally be neglected. As a concrete example, an arrangement of 18.5 periods of $Al_{0.86}Ga_{0.14}N$ (172nm)/GaN(78nm) tunes the FF at 1064nm and the SH at 532nm with an incidence angle for the FF at 39° as indicated in Fig. 4.

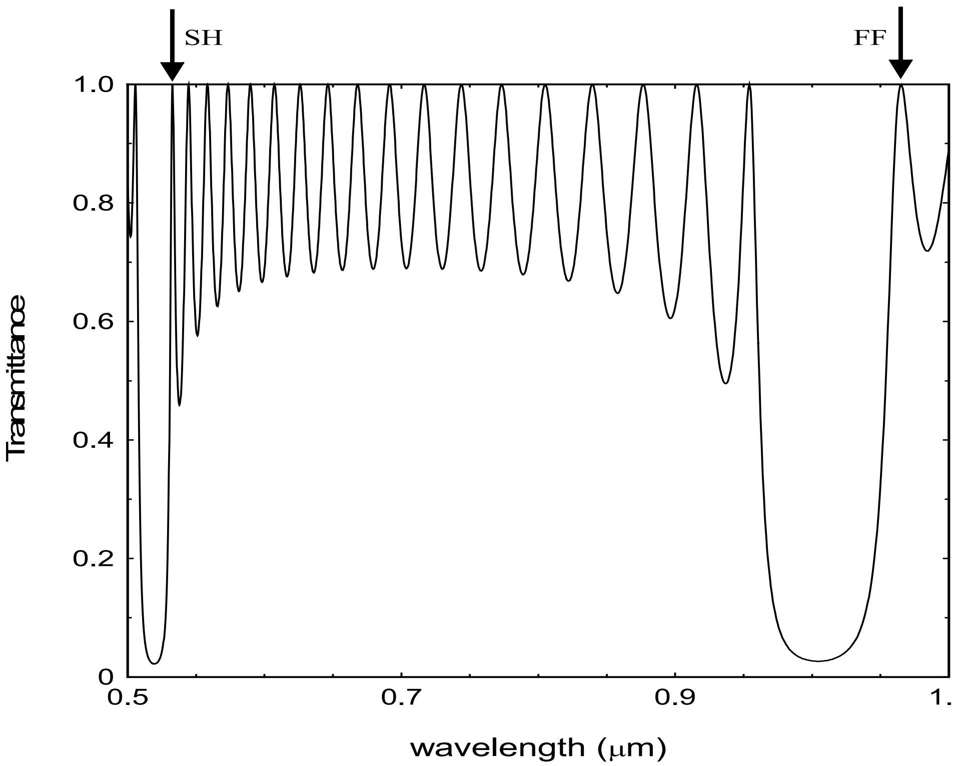

Figure 4: Trasmission spectrum vs wavelenght for the 18,5 period $Al_{0.86}Ga_{0.14}N$ (172nm)/GaN(78nm) structure at 39° incidence angle. Both the FF (1064 nm) and SH (532 nm) are tuned to the band edge resonances as labeled by arrows.

5. CONCLUSIONS

In conclusion, it is possible to take full advantage of field localization effects in such a way to weaken the role played by effective PM conditions in the nonlinear dynamics. We showed that higher SH generation conversion efficiency is achieved when the fast varying terms in the nonlinear polarization related to the presence of counter-propagating waves are not negligible, and by properly tailoring the size and distribution of the nonlinear layers in spite of fulfilling PM conditions.

Two of us (M.C. and G.D.) wish to acknowledge the U.S. Army European Research Office for partial financial support.

REFERENCES

1] R. Boyd, Nonlinear Optics 2nd edition, Academic Press, INC; (2002)
2] A. Yariv, Quantum electronics 3rd edition, John Wiley & Sons;(1989)
3] M. Centini, C. Sibilia, M. Scalora, G. D'Aguanno, M. Bertolotti, M. J. Bloemer, C. M. Bowden, and I. Nefedov. Phys. Rev. E **60**, 4891 (1999)
4] Y. Dumeige, I. Sagnes, P. Monnier, P. Vidakovic, I. Abram, C. Mériadec, and A. Levenson Phys. Rev. Lett. 89, 043901 (2002)
5] A. Melloni, F. Morichetti, and M. Martinelli Opt. Photon. News 14, 44 (2003)
6] G. D'Aguanno, M. Centini, M. Scalora, C. Sibilia, M. Bertolotti, M. J. Bloemer, and C. M. Bowden J. Opt. Soc. Am. B **19**, 2111 (2002)
7] J. Khurgin, J. Appl. Phys. **64**, 10 (1988)
8] A. Fiore, S. Janz, L. Delobel, P. van der Meer, P. Bravetti, V. Berger, E. Rosencher, J. Nagle Appl. Phys. Lett. **72**, 23 (1998)